



1                   **The current sheet flapping motions induced by**  
2 **non-adiabatic ions: case study**

3

4 **Xinhua Wei<sup>1</sup>, Chunlin Cai<sup>1</sup>, Henri Rème<sup>2</sup>, Iannis Dandouras<sup>2</sup>, George Parks<sup>3</sup>**

5

6 1 State Key Laboratory of Space Weather, National Space Science  
7 Center, CAS, Beijing, China

8 2 IRAP, UPS-OMP, Université de Toulouse, CNRS, Toulouse, France

9 3 Space Sciences Laboratory, University of California, Berkeley,  
10 California, USA

11

12

13

14

15

16

17

18

19

20

21

22



23 **Abstract**

24 In this paper, we analyzed the y-component of magnetic field line curvature in the  
25 plasma sheet and found that there are two kinds of shear structures of the flapping  
26 current sheet, i.e. symmetric and antisymmetric. The alternating bending orientations  
27 of guiding field are exactly corresponding to alternating north-south asymmetries of  
28 the bouncing ion population in the sheet center. Those alternating asymmetric plasma  
29 sources consequently induce the current sheet flapping motion as a driver. In addition,  
30 a substantial particle population with downward motion was observed in the center of  
31 a bifurcated current sheet. This population is identified as the quasi-adiabatic particles,  
32 and provides a net current opposite to the conventional cross-tail current.

33

34

35

36

37

38

39

40

41

42

43

44



## 45 **1. Introduction**

46 The magnetotail current sheet, which separates the northern lobe of the magnetotail  
47 from the southern lobe, is one of key objects of magnetospheric physics. As early as  
48 in 1967, the magnetotail current sheet was observed to move in the north-south  
49 direction [Speiser and Ness, 1967], which has been referred to as flapping motions  
50 [Lui et al., 1978; Sergeev et al., 1998]. Previous studies based on single-spacecraft  
51 measurements show that the geometry of the flapping current sheet is more complex  
52 than a planar surface, and that the sheet may be wavy [Lui et al., 1978; Nakagawa and  
53 Nishida, 1989].

54 The multi-point Cluster spacecraft have provided the chance to distinguish the spatial  
55 and time resolutions of the current sheet flapping. In the past two decades, intense  
56 investigations using Cluster data were performed to analyze the magnetic and current  
57 structures of the flapping current sheet. The flapping motion of the current sheet is  
58 interpreted as large amplitude waves with periods from about 30s to several minutes  
59 and amplitudes from several nT to dozens of nT [Zhang et al., 2005, 2006; Runov et  
60 al., 2003, 2005; Sergeev et al., 2003; Cai et al., 2008]. The flapping wave propagates  
61 from the central sector of the magnetotail toward the flanks [Sergeev et al, 2004], and  
62 the propagation velocities of waves are in the range of several tens km/s for the  
63 locally quiet sheets, and up to 200km/s during fast flows. Runov et al. [2005]  
64 performed a statistical analysis of the electric current and magnetic field geometries of  
65 flapping magnetotail current sheets during the period from July to October 2001.  
66 Their results show that  $J_z$  is often larger than  $J_y$  and the current is almost vertical, and



67 the flapping current sheet strongly deviates from the nominal plane geometry. The  
68 flapping waves can extend over  $\sim 10 R_e$  in the sun-earth direction by comparing the  
69 data from the Cluster and Double Star missions [Zhang et al, 2005]. In addition, the  
70 joint observations of THEMIS and Cluster show that the flapping amplitude of the  
71 current sheet is from 1 to  $3 R_e$  [Runov et al, 2009], and the flapping waves are steep  
72 tail-aligned structures with a longitudinal scale of  $>10 R_e$ .

73 The triggering mechanism of current sheet flapping looks rather mysterious. Early  
74 researchers suggest that flapping motions of the tail plasma sheet can be induced by  
75 the interplanetary magnetic field variations [Toichi Tsutomu and Miyazaki Teruki  
76 1976]. The solar wind dynamic pressure pulse and substorm are also considered to be  
77 the sources of flapping waves [Forsyth et al., 2009]. Some current sheet flapping  
78 events were often observed in association with magnetospheric activities. In 1976,  
79 Toichi and Miyazaki found that current sheet flapping motions occur during the early  
80 phases of substorms. Sergeev et al [1998] showed that current sheet flapping events  
81 are observed around substorm onsets while Sergeev et al. [2006], utilizing the Geotail  
82 data, showed that the majority of fast crossings of the current sheet occurred during  
83 the period of low magnetic activities. Thus, the relationship of the substorm and the  
84 current sheet flapping is still unclear. The flapping wavy motions can also be  
85 generated by the Kelvin-Helmholtz instability in the presence of dawn-dusk flows  
86 with a speed of several tens of km/s are present [Nakagawa and Nishida, 1989].  
87 Furthermore, when hot magnetospheric plasma is confined in a curvilinear magnetic  
88 field, the ballooning mode instability is also able to excite the flapping motion



89 [Golovchanskaya and Maltsev, 2005]. But this condition can't be often satisfied. The  
90 flapping wavelength can usually achieve 4 ~8  $R_E$ , while the curvature radius of  
91 magnetic field lines within the current sheet is only of 0.7-1.8  $R_E$ . In addition, there  
92 are often some transient events in the tail plasma sheet, such as bursty bulk flow  
93 [Angelopoulos et al., 1992; Baumjohann et al., 1990; Cao et al., 2006, 2013]. Some  
94 current sheet flapping events were observed to be associated with these fast flows  
95 [Sergeev et al, 2006; Duan et al., 2013]. Their flapping velocities are smaller (several  
96 tens of kilometers per second) in the slow-flow regions.

97 Kink-like MHD waves have been considered as the generation mechanism of the  
98 flapping motion [Daughton, 1999; Fruit et al., 2002, 2004]. Their phase speeds are  
99 usually more than hundreds km/s and are not consistent with the flapping wave  
100 propagating speeds of tens km/s [Sergeev et al., 2004]. Taking account of kinetic  
101 effects, some models investigated drift K-H instabilities spreading with ion drift  
102 speeds [Lapenta et al., 1997; Karimabadi et al., 2003]. Although these waves have  
103 comparable propagation speeds, their propagation directions are unidirectional and  
104 also don't match with the observations. Malova et al [2007] analyzed an asymmetric  
105 current sheet model and suggested that hemispheric asymmetric plasma sources can  
106 induce the flapping motions. Recently, Wei et al. [2015], using Cluster data,  
107 demonstrated that current sheet flapping motions are closely related to periodic  
108 hemispheric-asymmetric populations of bouncing particles. Their results imply that  
109 the specific nonadiabatic ion behaviors inside the central plasma sheet may excite the  
110 current sheet flapping motions.



111 In the sharp field reversal of the magnetotail current sheet, distinct classes of particle  
112 orbits can be organized using the  $\kappa$  parameter introduced by Büchner and Zelenyi  
113 [1986, 1989]. The  $\kappa$  parameter is defined as  $\kappa = (R_c / \rho_i)^{1/2}$ , where  $R_c$  is the minimum  
114 curvature radius of the magnetic lines and  $\rho_i = (2kT_i/m_i)^{1/2}/\omega_i$  is the maximum ion  
115 gyroradius. At large (above  $\sim 3$ )  $\kappa$  values, the particles motion is adiabatic, and the  
116 guiding center approximation is valid. For  $\kappa$  is between  $\sim 1$  and  $\sim 3$ , particles behave in  
117 a chaotic manner and their motion cannot be characterized by an invariant [Büchner  
118 and Zelenyi, 1989]. For  $\kappa < 1$ , those particles possibly meander inside the current sheet  
119 [Speiser, 1965] and exhibit either transient, trapped, or quasi-trapped behaviors [Chen  
120 and Palmadesso, 1986; Chen et al., 1990; Chen, 1992].

121 Furthermore, in the presence of a guiding field, the shear patterns of the magnetotail  
122 current sheet in association with the non-adiabatic particle kinetic can be strongly  
123 changed. Previous investigations on the non-adiabatic particles in the case of a  
124 constant  $B_y$  have been executed by both analytic methods and test particle simulations  
125 [Zhu and Park, 1993; Delcourt et al., 1996; Malova et al., 2012; Grigorenko et al.,  
126 2013]. These results revealed that asymmetrical particle scattering can take place in  
127 the vicinity of the neutral line. Particularly, Delcourt and Martin [1994] suggested an  
128 impulsive centrifugal force model to describe the nonadiabtic particle behaviors in the  
129 current sheet. In the presences of a guiding field, the effect of a nonzero  $B_y$  is  
130 considered to impart a rotation of the impulse centrifugal force when particles cross  
131 the neutral line [Delcourt et al., 1996]. It can be enhanced or attenuated when the  
132 rotation occurs along (against) the particle gyromotion [Delcourt et al., 1996, 2000].



133 Hence, particles launching from the north part of the current sheet will behave  
134 differently from that launching from the south part when they cross the central line.  
135 Meanwhile, the studies of magnetic configurations with a non-constant  $B_y$  and the  
136 associated non-adiabatic particle behaviors to reveal the formation of two general  
137 self-organized shear structures, symmetric and antisymmetric respectively [Malova et  
138 al., 2015].

139 In addition, due to their distinct motion behaviors, different classes of particles within  
140 the plasma sheet are supposed to have different capabilities of carrying cross-tail  
141 current. Thus, the particle population variations of different classes can change the  
142 current structure of the current sheet. For the adiabatic trapped ions, theoretically they  
143 do not carry any net current because their orbits are closed. Owing to strongly curved  
144 serpentine-like motions near the neutral plane, the quasi-adiabatic particles can  
145 support local currents that are directed oppositely to the general cross-tail current  
146 [Zelenyi et al., 2000, 2002a, b, 2003, 2011]. Thus, the existence of prominent  
147 populations of quasi-adiabatic particles will result in a current sheet with a bifurcated  
148 profile [Zelenyi et al., 2003]. The magnetic field of a bifurcated current sheet has a  
149 plateau profile between the peaks of the enhanced magnetic field gradient [Sergeev et  
150 al., 1993, 2003]. Bifurcated current sheets are often observed during substorms  
151 [Sergeev et al., 1993; Hoshino et al., 1996; Asano, 2001; Asano et al, 2003; Runov et  
152 al., 2003a]. In addition, bifurcated current sheets can exist around the X line, with a  
153 flat current sheet in between [Runov et al., 2003b].



154 In this paper, we reveal the symmetric and antisymmetric shear structures associated  
155 with the flapping current sheet. The alternating bending orientations of the guiding  
156 field are exactly corresponding to alternating North-South asymmetries of the  
157 bouncing ion population in the sheet center. In addition, we present the existence of a  
158 substantial population with dawnward motion in the center of a bifurcated current  
159 sheet, which is identified as the quasi-adiabatic particles.

160

## 161 **2. Observations**

162 2.1 flapping current sheet with antisymmetric shear structures: 03 Aug 2004 event and  
163 03 Aug 2001 event

164 Cluster satellites once observed long-standing flapping motions on 3 August, 2004  
165 when they traveled in the central current sheet. Those flapping motions were  
166 measured without notable fast flows (for the details, see Wei's et al., (2015) (Fig.2 a,  
167 d)). Figure 2 shows the measurements of the first five current sheet crossings during  
168 the period of 06:30-07:05UT, within which each encounter of the neutral line is  
169 marked by vertical dotted line. As revealed by pervious investigations [Runov et al.,  
170 2005; Petrukovich et al., 2006, 2008], although the current sheet inclined significantly  
171 in association with the flapping motions, the magnetic fields in the central current  
172 sheet are nearly unchanged and mainly in the z-direction.

173 Fig.3 shows the energy and polar angle spectrograms of energetic ions, which were  
174 measured by the CIS/HIA experiment [Rème et al., 2001]. The polar angle is the





175 angle between the particle movement direction and  $Z_{GSM}$  axis, in which  $\pm 90^\circ$   
176 represent the direction parallel and antiparallel to  $Z_{GSM}$  axis, respectively. First, during  
177 each crossing of the current sheet center, there are periodic variations of the ion flux  
178 concentrated at  $\pm 90^\circ$  polar angle respectively. In the magnetotail configuration, this  
179 observation means that the bouncing ion populations are North-South asymmetrical.  
180 For example, at the first crossing of the current sheet center, the ion flux moving  
181 upward is  $\sim 8 \times 10^4$  count/spin, while the flux moving downward is  $\sim 10^5$  count/spin.  
182 Second, these North-South asymmetries of the ion fluxes are alternating between the  
183 adjacent crossings of the sheet center. When the current sheet moved downward, the  
184 ion fluxes moving northward are smaller than that moving southward. While when the  
185 current sheet moved upward, the asymmetries are exactly in the opposite, that is, the  
186 ion fluxes moving northward are larger than that moving southward. Third, as shown  
187 in Fig.3c, there are polarization variations of  $\gamma_{cy}$  (the y-component of the magnetic  
188 field line curvature) measured at the current sheet center. The non-zero  $\gamma_{cy}$  is a  
189 manifestation of the bending of the magnetic field line to the y-direction developed in  
190 the current sheet center in association with its flapping motion. The sign change of  $\gamma_{cy}$   
191 means an orientation change of the field line curvature y-component, where the field  
192 line shape has an antisymmetric configuration (or in other words, an antisymmetric  
193 shear structure, see the schematic Fig.1a or Figure 4b in Malova et al, 2015).  
194 Although at the first look, all the polarization variations of  $\gamma_{cy}$  seem to have similar  
195 profiles, in fact, the polarization variations are alternating. For example at the first  
196 crossing of the current sheet center,  $\gamma_{cy}$  changes from negative to positive, where its



197 negative (positive) value corresponds to negative ( positive )  $B_x$  respectively.  
198 However at the next crossing, although  $\gamma_{cy}$  also changes from negative to positive, its  
199 negative (positive) value corresponds to positive (negative)  $B_x$  respectively. Thus, the  
200 bending in the y-direction of the magnetic field lines measured at the first crossing is  
201 actually opposite to the bending direction of the next crossing and so on for  
202 subsequent crossings. Alternating orientations of the adjacent crossings are presented  
203 as the solid line and the dashed line respectively in Fig. 1a. This picture of the  
204 antisymmetric orientation changes of the magnetic field line curvature in the  
205 y-direction can also be equivalently interpreted as an effective guiding field existing  
206 near the current sheet center due to its alternating inclinations [Wei et al, 2015].  
207 The particle motion in the magnetotail configuration is usually classified by its  
208 adiabaticity parameter. In this event, the adiabaticity parameter  $\kappa = (R_c / \rho_i)^{1/2} \sim 1.1$ ,  
209 where  $R_c \sim 2000$  km, is the curvature radius and  $\rho_i \sim 1600$  km, is the ion gyroradius.  
210 As mentioned above, the nonadiabtic particle behavior can be affected by the guiding  
211 fields, which result in the asymmetrical particle scattering in the vicinity of the neutral  
212 line. Especially, it is convenient to consider it as the existence of an impulse  
213 centrifugal force due to the field line curvature y-component. Therefore, a series of  
214 alternating hemispheric asymmetric ion populations can develop due to the  
215 occurrence of the alternating orientations of the field line bending in the y-direction.  
216 Theoretically, asymmetric plasma sources will violate the pressure balance condition  
217 of the current sheet in the North-South direction and consequently drive the sheet to  
218 reach a new equilibrium position [Malova et al., 2007]. Furthermore, this process is



219 self-consistent to preserve a complete flapping period. In the first half of a flapping  
220 period, asymmetric plasma sources developed due to a specific orientation of the field  
221 line bending and drove a vertical motion of the current sheet. Meanwhile, they reform  
222 the shear configuration of the current sheet, i.e., the field line bending in the  
223 y-direction, to the opposite orientation. In the second half of the flapping period,  
224 opposite asymmetric plasma sources were caused by guiding fields with an opposite  
225 bending orientation, and in their turn propel the current sheet to move vertically in the  
226 opposite direction. Thus, the alternating asymmetric plasma sources maintain the  
227 continuous oscillations of the current sheet. ( See the schematic Figure 1b in Wei et al,  
228 2015).

229 A similar event of the current sheet flapping with antisymmetric shear structures is  
230 shown in Figure 4. Two crossings of the neutral line during the period of  
231 09:00-09:25UT on Aug 3 2001 were recorded. There are no high speed flows during  
232 this current sheet flapping event (not showing in Fig.4). The ion flux moving upward  
233 ( $1.3 \times 10^5$  count/spin) is larger than that moving downward ( $1.0 \times 10^5$  count/spin) at the  
234 first travel through the neutral line, while the flux moving upward ( $1.0 \times 10^5$  count/spin)  
235 are smaller than that moving downward ( $1.4 \times 10^5$  count/spin) at the second travel  
236 through. Corresponding to the alternating asymmetric ion fluxes, the alternating  
237 orientations of the field line bending in the y-direction were measured as shown in Fig.  
238 4c. In the first crossing of the current sheet center, the field line bending is to the  
239 negative y-direction in the north-hemisphere and positive y-direction in the  
240 south-hemisphere. While in the second crossing, the bending is to the positive



241 y-direction in the north-hemisphere and negative y-direction in the south-hemisphere.  
242 In this event, the adiabaticity parameter  $\kappa = (R_c / \rho_i)^{1/2} \sim 1.05$ , where  $R_c \sim 1000\text{km}$ , and  
243  $\rho_i \sim 900\text{km}$ . As expected,  $\kappa$  is within  $\sim 1\text{-}3$  regime, so that the bouncing particles  
244 behave in a chaotic manner in the vicinity of the neutral line and experience  
245 asymmetric scattering. All the observational features can be interpreted as the same as  
246 the above event.

247

248 2.2 Bifurcated flapping current sheet with symmetric shear structures: 26 Sept  
249 2001 event

250 On 26 Sept 2001, during the period of 22:20-22:35 UT, Cluster observed a bifurcated  
251 flapping current sheet event when they was located at  $[-18; 7; 0] R_E$  (in GSM  
252 coordinates), which had been previously reported by Sergeev et al [2003]. Figure 5  
253 displays an overview of this event, in which no remarkable bulk burst flows were  
254 encountered. As shown in Fig.5a, during each crossing of the sheet center,  $B_x$  displays  
255 a plateau profile, which is more easily identified during the last four crossings.  
256 Correspondingly, the maximum cross-tail current  $j_y$  deviates from the exact center of  
257 the current sheet as shown in the third panel, that is, the total  $j_y$  does indeed decrease  
258 in the exact current sheet center and sometime displays a double-peak profile.

259 In association with the flapping motion of this bifurcated current sheet, alternating  
260 hemispheric asymmetries of the bouncing ion population can as well be observed as  
261 shown in Fig.6b. Corresponding to the hemispheric asymmetric of ion populations,  
262 non-zero values of  $\gamma_{ey}$  were observed during each crossing of the central current sheet.



263 Nevertheless, the measurements of the non-zero  $\gamma_{cy}$  are different to that of the events  
264 with antisymmetric shear structures. All these non-zero  $\gamma_{cy}$  don't change their signs at  
265 the crossing of the neutral plane, the non-zero  $\gamma_{cy}$  without a sign change represents a  
266 symmetric bending shape of the field lines in the y-direction (see the schematic Fig.  
267 1b, or Figure 4a in Malova et al, 2015). Similarly, as shown as the solid and dashed  
268 lines respectively in Fig.1b, the orientations of the bending shapes are alternating  
269 between the adjacent crossings of the sheet center, that is,  $\gamma_{cy}$  is positive when the  
270 current sheet moved upward, while is negative when the current sheet moved  
271 downward. Here, the adiabaticity parameter  $\kappa = (R_c / \rho_i)^{1/2} \sim 0.9$ , where  $R_c \sim 500\text{km}$ ,  
272 and  $\rho_i \sim 540\text{km}$ . Thus, asymmetric ion populations are supposed to develop due to the  
273 alternating orientations of the bending shapes in the y-component.

274 Fig. 6c shows the azimuthal angle spectrograms of energetic ions. The azimuthal  
275 angle ( $-180^\circ - +180^\circ$ ) is the angle between the particle movement direction and X  
276 axis, in which  $0^\circ$  represents the +x-direction, and  $\pm 90^\circ$  represents the direction  
277 parallel and antiparallel to y-axis respectively. During each crossing of the sheet  
278 center except the first two, the angular distribution of a substantial population is  
279 concentrate at  $-90^\circ$ , which means that this population move to the -y-direction,  
280 namely to the dawn direction. It is worth to note here that this particular observation  
281 are rare and cannot be found in the above events (not shown in this paper). In this  
282 event, the adiabaticity parameter  $\kappa \sim 0.9 < 1$ , thus it is reasonable to believe that a part  
283 of the nonadiabatic ions belongs to the so called quasi-adiabatic particles. Those  
284 particles meander in the current sheet center, and have a drift motion in the



285 -y-direction owing to their strongly curved serpentine-like motions near the neutral  
286 plane. Thus, this population carries a net current opposite to the cross-tail current in  
287 the sheet center. Consequently, the total cross-tail current carried by the whole  
288 population will decrease in the sheet center and display a bifurcated profile, that is,  
289 the current density maximum is not at the sheet center as the usual Harris-type sheet.  
290 Here, the fact that there exists a substantial population with downward motion in a  
291 bifurcated current sheet gives a firm observational evidence for its theoretical  
292 generation mechanism.

293

### 294 2.3 Flapping current sheet with mixed shear structures: 26 Oct 2002 event

295 Bulk burst flows are common phenomena in the magnetotail. Figure 7 shows the  
296 overview of a flapping current sheet with high speed flows observed by C3 on 26 Oct  
297 2002. There are 8 crossings of the current sheet center during the period of  
298 09:18-09:28UT. The periods of current sheet flapping are less than 2 minutes.  
299 Apparent earthward fast flows were observed during this current sheet flapping event  
300 as shown in Fig. 7d. The maximum high speed flow  $V_x$  is larger than 400km/s, which  
301 encountered at the seventh crossing. The burst feature of this flow can be found from  
302 the observations that the flows encountered at the second and seventh crossings are  
303 remarkable, while the ones encountered at the fourth and fifth crossings are ignorable.

304 In this flapping current sheet with high speed flows, the alternating hemispheric  
305 asymmetries of the bouncing ion population can also be recognized as shown in  
306 Fig.8b. However, the asymmetries recorded at the upward motions of the current sheet



307 seem to be more pronounced than the ones recorded at the downward motions, except  
308 the last one. Meantime, the upward amplitudes of the current sheet flapping seem to  
309 also be more pronounced than the downward amplitudes, except the last two flapping  
310 motions. Two populations concentrated at  $0^\circ$  polar angle were encountered between  
311 the second and third crossings and at the seventh crossing, which are the earthward  
312 fast flows. Corresponding to the hemispheric asymmetric of ion populations, non-zero  
313 values of  $\gamma_{cy}$  were observed in the vicinity of the neutral line. Beside the non-zero  $\gamma_{cy}$   
314 with a sign change, the non-zero  $\gamma_{cy}$  without a sign change was recorded at the second,  
315 fourth and sixth crossings of the sheet center. Thus, the shear structures in this event  
316 are mixed, i.e. both symmetric and antisymmetric bendings are existed. It is contrast  
317 to the events presented above, where all the non-zero  $\gamma_{cy}$  have similar profiles. In  
318 this event, the adiabaticity parameter  $\kappa = (R_c / \rho_i)^{1/2} \sim 1.8$ , where  $R_c \sim 1000\text{km}$ , and  
319  $\rho_i \sim 315\text{km}$ . Although the magnetic structures with fast flows are more complex than  
320 that of the case without fast flows, the intrinsic excitation mechanism of flapping  
321 motion induced by nonadiabatic ions are still prevailed.

322

### 323 **3. Discussion and conclusion**

324 In association with the current sheet flapping motion, there are two type bending  
325 patterns of the field lines in the y-direction, symmetric and antisymmetric as revealed  
326 by the observations. In 03 Aug 2004 and 03 Aug 2001 events, the unperturbed  
327 magnetic fields in the current sheet center are mainly in the z-direction.  
328 Correspondingly, their bending patterns are antisymmetric. This picture can be



329 equivalently interpreted as an effective guiding field due to the inclinations of the  
330 current sheet itself (Wei et al, 2015). While in 26 Oct 2002 and 26 Sept 2001 events,  
331 both the z-component and y-component of the unperturbed magnetic fields are rather  
332 small. Correspondingly, their bending patterns are symmetric or complicated (two  
333 patterns coexist). Thus, we infer that in the case of an unperturbed magnetic field with  
334 a dominant z-component, it is favorable to develop an antisymmetric bending pattern  
335 of the field lines in the y-direction during the flapping motion, while in the other case;  
336 it is favorable to develop an antisymmetric bending pattern. It is consistent with the  
337 conclusion drew by the previous investigations that a higher probability of formation  
338 of symmetric shear configuration at lower values of the normal magnetic component  
339 [Rong et al., 2011; Malova et al., 2015].

340 Although an understanding of the asymmetric particle scattering of the bouncing ion  
341 populations by guiding fields has been pointed out in Wei et al (2015), the scenario  
342 shown here relevant to the detailed shear structures of the current sheet is more  
343 general since the two kinds of shear patterns are self-consistently formatted from  
344 some initial magnetic perturbation [Malova et al., 2015]. Also, in the view of an  
345 impulse centrifugal force model which is applicable to describe ion behaviors with  
346 adiabaticity parameter  $\kappa \sim 1-3$  as in the case of flapping events, it is more convenient  
347 to investigate directly the magnetic line curvature rather than an effective guiding  
348 field.

349 In summary, observations of flapping current sheet in the magnetotail are presented to  
350 reveal their intrinsic excitation mechanism induced by nonadiabatic ions. The current





351 sheet up-down motions are exactly corresponding to alternating hemispherical  
352 asymmetries of the bouncing ion population. These asymmetric ion populations are  
353 present in the magnetic field configuration with a local bending y-component and  
354 interpreted as a result of the nonadiabatic particle scattering in the vicinity of the  
355 neutral line. Hence, the alternating asymmetric ion populations can develop due to the  
356 occurrence of the alternating orientations of the field line bending. Those alternating  
357 asymmetric plasma sources consequently induce the current sheet flapping motion as  
358 a driver. In addition, we present the observations that there exists a substantial  
359 population with downward motion in the center of a bifurcated current sheet. This  
360 population is identified as the quasi-adiabatic particles, which supports a net current  
361 opposite to the cross-tail current. The present results suggest that nonadiabatic ions  
362 play a substantial role to determine current sheet dynamics, both its bulk mechanical  
363 instability and current profiles.

364

365

366

367

368

369

370

371

372



373 **Acknowledgements**

374 This work is supported by the National Natural Science Foundation of China (NSFC)  
375 under Grant No. 41174144 and 40974098 and the Specialized Research Fund for State  
376 Key Laboratories. Cluster data used in this paper are available via the Cluster Science  
377 Archive (<https://www.cosmos.esa.int/web/csa/>).

378

379 **References**

- 380 Angelopoulos, V., W. Baumjohann, C. F. Kennel, et al.: Bursty bulk flows in the inner  
381 central plasma sheet, *J. Geophys. Res.*, *97*, 4027, 1992
- 382 Asano, Y.: Configuration of the thin current sheet in substorms, Ph.D. thesis, Univ. of  
383 Tokyo, Tokyo, 2001
- 384 Asano, Y., T. Mukai, M. Hoshino, Y. Saito, H. Hayakawa, and T. Nagai: Evolution of  
385 the thin current sheet in a substorm observed by Geotail, *J. Geophys. Res.*, *108*(A5),  
386 1189, doi:10.1029/2002JA009785, 2003
- 387 Baumjohann, W., G. Paschmann, H. Lühr: Characteristics of the high-speed flows in  
388 the plasma sheet, *J. Geophys. Res.*, *95*, 3801, 1990
- 389 Büchner, J., and L. M. Zelenyi: Deterministic chaos in the dynamics of charged  
390 particles near a magnetic field reversal, *Phys. Lett. A*, *118*, 395 – 399,  
391 doi:10.1016/0375-9601(86)90268-9, 1986
- 392 Büchner, J., and L. M. Zelenyi: Regular and chaotic charged particle motion in  
393 magnetotail-like field reversals: 1. Basic theory of trapped motion, *J. Geophys. Res.*,  
394 *94*, 11,821–11,842, 1989



- 395 Cai, C.L., I. Dandouras, H. Rème, J.B. Cao, G.C. Zhou, and G.K. Parks.: Cluster  
396 observations on the thin current sheet in the magnetotail, *Annales Geophysicae*, 26(4),  
397 929-940, SRef-ID: 1432-0576/ANGE0/2008-26-929, 2008
- 398 Cao, J. B., Y. D Ma, G. Parks, H. Reme, I. Dandouras, R. Nakamura, T. L.Zhang, Q.  
399 Zong, E. Lucek, C. M. Carr, Z. X. Liu and G. C. Zhou: Joint observations by Cluster  
400 satellites of bursty bulk flows in the magnetotail, *Journal of Geophysical*  
401 *Research-Space Physics*, 111(A4) A04206, doi:10.1029/2005JA011322, 2006
- 402 Cao, J. B., Y. Ma, G. Parks, H. Reme, I. Dandouras, and T. Zhang: Kinetic analysis of  
403 the energy transport of bursty bulk flows in the plasma sheet, *Journal of Geophysical*  
404 *Research-Space Physics*, A118(1),313-320, doi:10.1029/2012JA018351, 2013
- 405 Chen, J., and P. J. Palmadesso: Chaos and nonlinear dynamics of single-particle orbits  
406 in magnetotail like magnetic field, *J. Geophys. Res.*,91, 1499, 1986
- 407 Chen, J., G. R. Burkhart, and C. Y. Huang: Observational signatures of nonlinear  
408 magnetotail particle dynamics, *Geophys. Res. Lett.*, 17, 2237, 1990
- 409 Chen, J.: Nonlinear dynamics of charged particles in the magnetotail. *J. Geophys.*  
410 *Res.*,97, 15,011–15,050, doi:10.1029/92JA00955, 1992
- 411 Duan A.Y, J. B Cao, Y. D Ma, X. H Wei: Cluster observations of large-scale  
412 southwardmovement and dawnward-duskwaflapping of Earth's magnetotail current  
413 sheet, *Science in China(E)*, 56 (1), 194–204, 2013
- 414 Daughton, W.: The unstable eigenmodes of a neutral sheet. *Phys.Plasmas*, 6, 1329,  
415 1999
- 416 Delcourt, D.C., and R. F. Martin Jr: Application of the centrifugal impulse model  
417 toparticle motion in the near-Earth magnetotail . *J. Geophys. Res.*, 99, 23,583, 1994
- 418 Delcourt et al.: Centrifugally driven phase bunching and related current sheet



419 structure in the near-Earth magnetotail, J. Geophys. Res. 101, 19839–19847, 1996

420 Delcourt, D. C., L. M. Zelenyi, and J.-A. Sauvaud: Magnetic moment scattering in a  
421 field reversal with nonzero  $B_y$  component. J. Geophys. Res., 105,  
422 349–360, doi:10.1029/1999JA900451, 2000

423 Forsyth et al.: Solar wind and substorm excitation of the wavy current sheet, Ann  
424 Geophys, 327, 2457–2474, 2009

425 Fruit, G., P. Louarn, A. Tur, and D. Le Queau: Propagation of MHD perturbations in a  
426 Harris current sheet: 1. Discrete modes. J. Geophys. Res., 107(A11),  
427 1411, doi:10.1029/2001JA009212, 2002

428 Fruit, G., et al.: On the propagation of low frequency fluctuations in the plasma  
429 sheet: 2. Characterization of the MHD eigenmodes and physical implication. J.  
430 Geophys. Res., 109, doi:10.1029/2003JA010229, 2004

431 Golovchanskaya and Maltsev: On the identification of plasma sheet flapping waves  
432 observed by Cluster. J. Geophys. Res., 32, L17S13, 2005

433 Grigorenko, E. E., et al.: Current sheet structure and kinetic properties of plasma  
434 flows during a near-Earth magnetic reconnection under the presence of a guide field,  
435 *Journal of Geophysical Research-Space Physics*, 118, 3265–3287,  
436 doi:10.1002/jgra.50310, 2013

437 Hoshino, M., A. Nishida, T. Mukai, Y. Saito, T. Yamamoto, and S. Kokubun:  
438 Structure of plasma sheet in magnetotail: Double-peaked electric current sheet, J.  
439 Geophys. Res., 101, 24,775, 1996

440 Karimabadi, H., W. Daughton, P. L. Pritchett, and D. Krauss-Varban: Ion-ion kink



441 instability in the magnetotail: 1. Linear theory. J. Geophys. Res., 108(A11),  
442 1400,doi:10.1029/2003JA010026, 2003

443 Lapenta, G, and J. U. Brackbill: A kinetic theory for the drift-kink instability.  
444 J.Geophys. Res., 102, 27,099, 1997

445 Lui et al.: Wavy nature of the magnetotail neutral sheet. Geophys. Res. Lett., 5,  
446 279-282, 1978

447 Malova, H. V., L. M. Zelenyi, V. Popov, D. Delcourt, A. Petrukovich, and A. Runov:  
448 Asymmetric thin current sheets in the Earth's magnetotail. Geophys. Res. Lett.,  
449 34,L16108, doi:10.1029/2007GL030011, 2007

450 Malova, H. V., et al.: Thin current sheets in the presence of a guiding magnetic field in  
451 Earth's magnetosphere. J. Geophys. Res., 117, A04212, doi:10.1029/2011JA017359X,  
452 2012

453 Malova, H. V., et al.: Formation of self-organized shear structures in thin current  
454 sheets, J. Geophys. Res. Space Physics, 120, 4800–4824, doi:10.1002/2014JA020974,  
455 2015

456 Nakagawa and Nishida: Southward magnetic field in the neutral sheet produced by  
457 wavy motions in the quiet plasma sheet, Ann Geophys,26: 3669-3676, 1989

458 Petrukovich, A.A., et al.: Oscillations of flux tube slippage in the quiet plasma  
459 sheet. Ann. Geophys. 24, 1695–1704, 2006

460 Petrukovich, A.A., et al.: Formation of current density profile in tilted current sheets.  
461 Ann. Geophys. 26, 3669–3676, 2008

462 Rème, H., et al.: First multispacecraft ion measurements in and near the Earth's



463 magnetosphere with the identical Cluster ion spectrometry (CIS) experiment. Ann.  
464 Geophys., 19, 1303, 2001

465 Rong, Z. J., W. X. Wan, C. Shen, X. Li, M. W. Dunlop, A. A. Petrukovich, T. L.  
466 Zhang, and E. Lucek: Statistical survey on the magnetic structure in magnetotail  
467 current sheets. J. Geophys. Res., 116, A09218, doi:10.1029/2011JA016489, 2011

468 Runov, A., R. Nakamura, W. Baumjohann, T. L. Zhang, M. Volwerk, H.-U.  
469 Eichelberger, and A. Balogh: Cluster observation of a bifurcated current sheet,  
470 Geophys. Res. Lett., 30(2), 1036, doi:10.1029/2002GL016136, 2003a

471 Runov, A., et al.: Current sheet structure near magnetic X line observed by Cluster,  
472 Geophys. Res. Lett., 30(11), 1579, doi:10.1029/2002GL016730, 2003b

473 Runov, A., et al.: Electric current and magnetic field geometry in flapping magnetotail  
474 current sheets. Ann. Geophys. 23, 1391–1403, 2005

475 Runov et al.: Global properties of magnetotail current sheet flapping: THEMIS  
476 perspectives. Ann. Geophys. 27, 319–328, 2009

477 Sergeev, V. A., Mitchell, D. G., Russell, C. T., and Williams, D. J.: Structure of the tail  
478 plasma/current sheet at 11  $R_E$  and its changes in the course of a substorm, J. Geophys.  
479 Res., 98, 17345–17366, doi:10.1029/93JA01151, 1993

480 Sergeev, V., V. Angelopoulos, C. Carlson, and P. Sutcliffe: Current sheet  
481 measurements within a flapping plasma sheet, J. Geophys. Res., 103, 9177– 9187,  
482 1998

483 Sergeev, V., et al.: Current sheet flapping motion and structure observed by Cluster.  
484 Geophys. Res. Lett. 30 (6), 1327, doi:10.1029/2002GL016500, 2003



- 485 Sergeev, V., et al.: Orientation and propagation of current sheet oscillations. *Geophys.*  
486 *Res. Lett.* 31, L05807, doi:10.1029/2003GL019346, 2004
- 487 Sergeev, V. A., Sormakov, D. A., Apatenkov, S. V., Baumjohann, W., Nakamura, R.,  
488 Runov, A., Mukai, T., and Nagai, T.: Survey of large-amplitude flapping motions in  
489 the midtail current sheet, *Ann. Geophys.*, 24, 2015–2024, 2006
- 490 Speiser, T. W.: Particle trajectories in model current sheets: 1. Analytical solutions, *J.*  
491 *Geophys. Res.*, 70, 4219 – 4226, 1965
- 492 Speiser and Ness: Particle trajectories in model current sheets: 2. Applications to  
493 auroras using a geomagnetic tail model, 72, 15, 3921-3932, 1967
- 494 Toichi Tsutomu and Miyazaki Teruki: Flapping motions of the tail plasma sheet  
495 induced by the interplanetary magnetic field variations. *Planet Space Sci.*, 24:147-159,  
496 1976
- 497 Wei, X. H., C. L. Cai, J. B. Cao, H. Rème, I. Dandouras, and G. K. Parks: Flapping  
498 motions of the magnetotail current sheet excited by nonadiabatic ions, *Geophysical*  
499 *Research Letters.*, 42, 4731–4735, doi:10.1002/2015GL064459, 2015
- 500 Zelenyi, L. M., M. I. Sitnov, H. V. Malova, and A. S. Sharma: Thin and superthin ion  
501 current sheets: Quasiadiabatic and nonadiabatic models. *Nonlinear Process. Geophys.*,  
502 7, 127–139, doi:10.5194/npg-7-127-2000, 2000
- 503 Zelenyi, L. M., M. S. Dolgonosov, A. A. Bykov, V. Y. Popov, and K. V. Malova:  
504 Influence of trapped plasma on the structure of collisionless thin current sheets,  
505 *Cosmic Res., Engl. Transl.*, 40, 357–366, doi:10.1023/A:1019846428446, 2002a
- 506 Zelenyi, L. M., D. C. Delcourt, H. V. Malova, and A. S. Sharma: “Aging” of the



507 magnetotail thin current sheets, *Geophys. Res. Lett.*, 29(12), 1608,  
508 doi:10.1029/2001GL013789, 2002b

509 Zelenyi, L. M., H. V. Malova, and V. Y. Popov: Bifurcation of thin current sheets in  
510 the Earth's magnetosphere, *Sov. Phys. JETP, Engl. Transl.*, 78, 296–299,  
511 doi:10.1134/1.1625728, 2003

512 Zelenyi, L. M., H. V. Malova, A. V. Artemyev, V. Y. Popov, and A. A. Petrukovich:  
513 Thin current sheets in collisionless plasma: Equilibrium structure, plasma instabilities,  
514 and particle acceleration. *Plasma Phys. Rep.*, 37, 118–160,  
515 doi:10.1134/S1063780X1102005, 2011

516 Zhang, T.L., et al.: Double Star/Cluster observation of neutral sheet oscillations on 5  
517 August 2004. *Ann. Geophys.* 23, 2909–2914, 2005

518 Zhang, T.L., et al.: A statistical survey of the magnetotail current sheet. *Adv. Space*  
519 *Res.* 38, 1834–1837, 2006

520 Zhu, Z., and G. Parks: Particle orbits in model current sheets with a nonzero By  
521 component. *J. Geophys. Res.*, 98, 7603, 1993

522

523

524

525

526

527

528





529 Figure Caption

530 Fig1. Schematic of field line shapes of the flapping current sheet. Alternating  
531 bendings in the y-direction of the adjacent crossings are presented as the solid line and  
532 the dashed line respectively. a) Antisymmetric. b) Symmetric.

533 Fig2. Detections of the flapping motion by the Cluster/C3 spacecraft on 3 August  
534 2004. a) The magnetic field in GSM coordinates. b) The density measurements of hot  
535 ions in the energy range of 5–40,000eV. c) The current and d) Plasma velocity.

536 Fig3. Ion observations of alternating hemispherical asymmetries of the bouncing ion  
537 population on 3 August 2004. a and b) The omnidirectional energy and polar angle  
538 spectrogram of hot ions, respectively. The values of  $\pm 90^\circ$  polar angle represent the  
539 direction parallel and antiparallel to Z axis, respectively. c) The magnetic field  
540 curvature y-component. d) current components and e) magnetic components.

541 Fig4. Ion observations of alternating hemispherical asymmetries of the bouncing ion  
542 population on 3 August 2001. a and b) The omnidirectional energy and polar angle  
543 spectrogram of hot ions, respectively. (c) The magnetic field curvature y-component.  
544 d) current components and e) magnetic components.

545 Fig5. Detections of the bifurcated flapping current sheet on 26 September 2001. a)  
546 The magnetic field in GSM coordinates. b) The density measurements. c) The current  
547 and d) Plasma velocity.

548 Fig6. Ion observations of alternating hemispherical asymmetries of the bouncing ion  
549 population and the dawnward moving population on 26 September 2001. a-c) The  
550 omnidirectional energy, polar angle and azimuthal angle spectrogram of hot ions,



551 respectively. The values of  $0^\circ$  azimuthal angle represents the +x-direction, and  $\pm 90^\circ$   
552 represent the direction parallel and antiparallel to y-axis respectively. d) The magnetic  
553 field curvature y-component. e) current components and f) magnetic components.

554 Fig7. Detections of the flapping motion with bulk flows on 26 October 2002. a) The  
555 magnetic field in GSM coordinates. b) The density measurements. c) The current and  
556 d) Plasma velocity.

557 Fig8. Ion observations of alternating hemispherical asymmetries of the bouncing ion  
558 population on 26 October 2002. a and b) The omnidirectional energy and polar angle  
559 spectrogram of hot ions, respectively. (c) The magnetic field curvature y-component.  
560 d) current components and e) magnetic components.

561

562

563

564

565

566

567

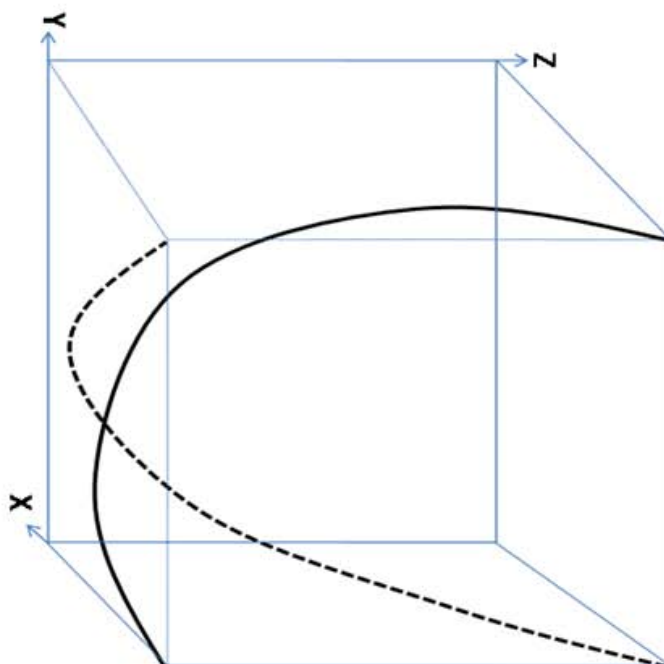
568

569

570



**a) Antisymmetric**



**b) Symmetric**

